# EPR of Yb$^{3+}$ ions in a monoclinic KY(WO$_4$)$_2$ single crystal

A.D. Prokhorov[1,2], M.T. Borowiec[1,a], M.C. Pujol[3], I.M. Krygin[2], A.A. Prokhorov[2], V.P. Dyakonov[1,2],
P. Aleshkevych[1], T. Zayarnyuk[1], and H. Szymczak[1]

[1] Institute of Physics, Polish Academy of Scences, Al. Lotników 32/46, 02-668, Warsaw, Poland
[2] A.A.Galkin Physico-Technical Institute, 340114 Donetsk, Ukraine
[3] Física i Cristal·lografia de Materials (FiCMA), Universitat Rovira i Virgili, Campus Sescelades C/ Marcel.lí Domingo,
S/N, 43007-Tarragona, Spain

**Abstract.** The electron paramagnetic resonance (EPR) of Yb$^{3+}$ ions in a KY(WO$_4$)$_2$ single crystal was
investigated at $T = 4.2$ K and fixed frequency of 9.38 GHz. The resonance absorption observed on the lowest
Kramers doublet represents the complex superposition of three spectra, corresponding to the ytterbium
isotopes with different nuclear moments. The EPR spectrum is characterized by a strong anisotropy of the
$g$-factors. The temperature dependence of the $g$-factors is shown to be caused by the strong spin-orbital
and orbital-lattice coupling. The resonance lines broaden with increasing temperature due to the short
spin-lattice relaxation times.

**PACS.** 75.30.Gw Magnetic anisotropy – 76.30.-v Electron paramagnetic resonance and relaxation

## 1 Introduction

The rare earth (RE) double tungstate crystals have been
synthesized for the fist time more than 30 years ago [1].
They are promising materials for stimulated radiation
light generation over a wide range of the frequencies. The
common scheme of laser generation channels for the ma-
jority of rare earth ions in a double tungstate matrix is
presented in reference [2]. The monoclinic KRE(WO$_4$)$_2$
tungstate also has sufficiently large optical nonlinearity to
be used in devices working on the basis of the compelled
Raman effect [3,4].

Investigations of RE double tungstates at low temper-
ature have revealed a series of interesting properties con-
nected with both magnetic and Jahn-Teller phase tran-
sitions, which for the first time were observed in the low
symmetry single crystals [5]. It is well known that the EPR
technique can be used to study the properties of the rare-
earth ion ground state in detail. To date, the EPR spectra
of the Gd$^{3+}$ [6], Dy$^{3+}$ [7], Er$^{3+}$ [8] and Nd$^{3+}$ [9] ions in
the magnetically diluted and concentrated single crystals
have been investigated. The following effects inherent to
low symmetry crystals were found:

(1) the main axes of the $g$-tensor do not coincide with
the crystallographic axes, and the orientations of the
$g$-tensor axis for each rare-earth ion are individual;
(2) there is poor agreement between the experimental res-
onance positions of the lines and the theoretical an-
gular dependence of resonance field extreme values in

the fine structure of EPR spectrum of the gadolinium
ion [6];
(3) in low symmetry double tungstates, the rare earth ions
are grouped in chains. The distance between nearest
magnetic ions in chains is less than the distance be-
tween chains [5];
(4) studies of spin-spin interaction in the Dy$^{3+}$ ion
pairs [9] as well as in magnetically concentrated
KDy(WO$_4$)$_2$ [10] show that besides dipolar interac-
tions, the exchange interactions including antisymmet-
ric exchange are meaningful;
(5) temperature dependence of the g-factor for
KY(WO$_4$)$_2$doped by the Dy$^{3+}$ and Er$^{3+}$ ions
was found.

This paper is a continuation of the EPR investigations of
the low symmetry double tungstates. The results of EPR
studies of diamagnetic KY(WO$_4$)$_2$ single crystal diluted
by a small concentration of the Yb$^{3+}$ ions are presented.

## 2 Crystal structure and experimental technique

The rare earth double tungstate KLn(WO$_4$)$_2$, where
Ln-Y, Gd-Lu, are related to the centrosymmetric 2/m
Laue class of the monoclinic singony. The structure
of potassium-yttrium tungstate was described in detail
in references [12,13], and the structure of isomorphic
potassium-gadolinium tungstate was determined in refer-
ences [14,15]. The structure of these crystals is described

$^a$ e-mail: borow@ifpan.edu.pl

by the two interconnected space groups: I2/c and C2/c. The lattice parameters of the unit cell for the I2/c and C2/c space groups are $a = 8.05$ Å, $b = 10.35$ Å, $c = 7.54$ Å and $\beta = 94°$ and $a_1 = 10.64$ Å, $b_1 = 10.35$ Å, $c_1 = 7.54$ Å and $\beta = 130.5°$, respectively. Basic vectors for the two space groups are connected by following relations: $a_1 = a + c; b_1 = -b; c_1 = -c$ [2,13]. The unit cell of the I2/c space group most corresponds to the habits of the crystal and, therefore, was used in the current work.

The yttrium ions occupy the $C_2$ point symmetry positions. They are located on double rotary axes surrounded by the eight oxygen ions. The edge bounded yttrium polyhedra form continuous chains along the $a$-axis. The potassium dodecahedra chains are parallel to them. The octahedron of six oxygen atoms are the nearest neighbors of the tungsten atoms. The tungstate-octahedra form continuous double chains along the $c$-axis. The trivalent rare earth ions replace the trivalent yttrium ions. In spite of the fact that the unit cell has four rare earth ions, they are magnetically equivalent in the I2/c space group, and as a result a single EPR spectrum is observed in the experiment.

The single crystals used in the EPR measurements were grown by spontaneous crystallization from the melt of $K_2W_2O_7$ by a slow decreasing of temperature from 1050 °C at a rate of 3 °C/h. After separation of crystals from solvent, the samples with a size of about 3 mm were selected. To establish the main axes of the $g$-tensor, the $ac$ plane should be determined, because the $g_x$- and $g_z$-axes lie in the $ac$ plane and the $g_y$-axis is directed along the $C_2$ symmetry axis, parallel to the $b$ crystallographic direction and perpendicular to the $ac$ plane. The concentrations of the $Yb^{3+}$ ions in the investigated single crystals were varied, being either 0.1% or 0.2%.

Measurements of EPR spectra were carried out using an X-band (Bruker made) spectrometer with high frequency modulation. The magnetic field was varied from 0 to 1 T. A flowing helium gas cryostat was used to change the sample temperature.

## 3 The angular dependence of the EPR spectra

The trivalent ytterbium ion ($Yb^{3+}$) has $4f^{13}$ electronic configuration with the ground multiplet $^2F_{7/2}$. The first excited multiplet $^2F_{5/2}$ is located $10^4$ cm$^{-1}$ above the ground multiplet. The low symmetry crystal field splits the ground multiplet into four Kramer doublets. According to optical measurements, in $KYb(WO_4)_2$ crystal these doublets are located as follows: 0, 168, 438 and 555 cm$^{-1}$ [16]. The $KYb(WO_4)_2$ and $KY(WO_4)_2$ double tungstates have identical structure and are isomorphic. Therefore we assume that the positions of excited levels in $Yb^{3+}$-doped $KY(WO_4)_2$ essentially do not depend on concentration, whether 0.1% or 0.2%.

The EPR spectrum observed on the lowest Kramers doublet represents the complex superposition of three spectra. It comes from the fact that natural ytterbium
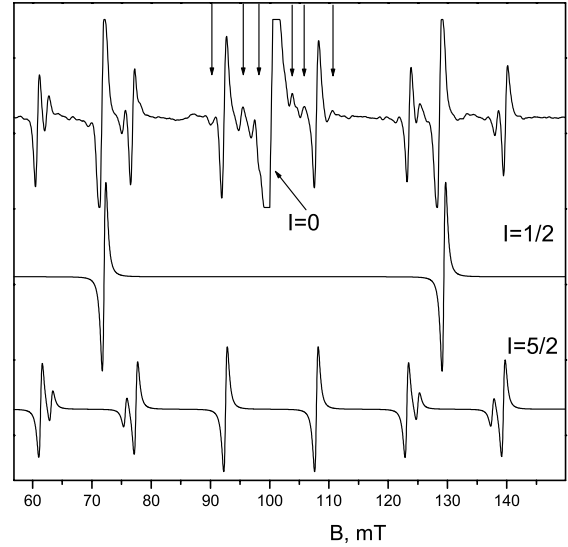


**Fig. 1.** The EPR spectrum of the $Yb^{3+}$ion in $KY(WO_4)_2$ for the $z$-orientation ($B||z$). The experimental spectrum is shown on the top of the figure. The intense line corresponds to the even isotope with $I = 0$. The calculated spectra for isotopes $Yb^{3+}$ (171) ($I = 1/2$) and $Yb^{3+}$ (173) ($I = 5/2$) are shown on the bottom. The arrows show lines not related to the single ion spectrum.

is a mixture of several isotopes with different nuclear moments. The nuclear moment is equal to zero for even isotopes (168–0.14%; 170–3.03%; 172–21.82%; 174–31.58%; 176–12.75%). The odd isotope number 171 with natural abundance of 14.38% has a nuclear magnetic moment of 0.493 $\mu_B$ and nuclear spin $I = 1/2$. Another odd isotope 173 (16.3%) has $I = 5/2$, magnetic moment of $-0.6725 \mu_B$ and quadrupolar moment of $3.9 \times 10^{-24}$ cm$^2$. As a result the hyperfine interactions of odd isotopes are essentially responsible for the complicated EPR spectrum. The EPR spectra of the $Yb^{3+}$ ion (at $T = 4.2$ K) along the $x, y,$ and $z$ orientations are presented in Figures 1–3, respectively. The $y$-axis coincides with the $C_2$ axis. The $z$ axis was chosen along the direction where the $g$-factor is maximal. The $z$ axis does not coincide with the crystallographic axis and, like the $x$ axis, is located in the $ac$ plane. According to the angular dependence of the spectrum measured in the $ac$ plane, the $z$ axis deviates from the crystallographic $c$ axis by an angle of $42° \pm 3°$. This direction coincides with the $z$ axis in $KYb(WO_4)_2$ [16].

The EPR spectra and their angular dependencies can be described by the following spin Hamiltonian [17]

$$\hat{H} = \beta \vec{B} g \hat{S} + \hat{S} A \hat{I} + \hat{I} P \hat{I} \qquad (1)$$

where $\beta$ is the Bohr magneton, $\vec{B}$ the magnetic induction vector, $g$ the spectroscopic splitting factor, $\hat{S}$ the electron spin operator, $\hat{I}$ the operator of nuclear spin, $A$ and $P$ are the tensors of hyperfine and quadrupolar interactions, respectively.

The experimentally determined parameters of the spin Hamiltonian (1) are presented in Table 1. The $A$ and $P$

**Table 1.** Experimentally determined parameters of the spin Hamiltonian.

| | $g_x$ | $g_y$ | $g_z$ | $A_{xx} \times 10^{-4}$ cm$^{-1}$ | $A_{yy} \times 10^{-4}$ cm$^{-1}$ | $A_{zz} \times 10^{-4}$ cm$^{-1}$ | $A_{xz} \times 10^{-4}$ cm$^{-1}$ | $P_{xx} \times 10^{-4}$ cm$^{-1}$ | $P_{yy} \times 10^{-4}$ cm$^{-1}$ | $P_{zz} \times 10^{-4}$ cm$^{-1}$ | $P_{zx} \times 10^{-4}$ cm$^{-1}$ |
|---|---|---|---|---|---|---|---|---|---|---|---|
| 0 | $0.959 \pm 0.001$ | $0.895 \pm 0.001$ | $6,64 \pm 0.01$ | | | | | | | | |
| 1/2 | $0.959 \pm 0.001$ | $0.895 \pm 0.001$ | $6,64 \pm 0.01$ | $251 \pm 1$ | $273 \pm 1$ | $1774 \pm 1$ | | | | | |
| 5/2 | $0.959 \pm 0.001$ | $0.895 \pm 0.001$ | $6,64 \pm 0.01$ | $71 \pm 2$ | $80 \pm 2$ | $479 \pm 0.5$ | $0$ | $5 \pm 1$ | $7.5 \pm 1$ | $51 \pm 2$ | $5 \pm 0.5$ |
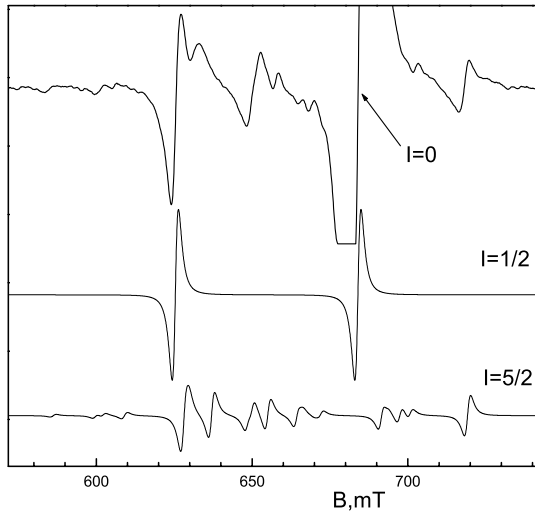


**Fig. 2.** The EPR spectrum of the Yb$^{3+}$ ion in KY(WO$_4$)$_2$ for the $x$-orientation ($B||x$). The experimental spectrum is shown on the top. The intense line corresponds to the even isotope with $I = 0$. The calculated spectra for isotopes Yb$^{3+}$ (171) ($I = 1/2$) and Yb$^{3+}$ (173) ($I = 5/2$) are shown on the bottom.



**Fig. 3.** The EPR spectrum of the Yb$^{3+}$ ion in KY(WO$_4$)$_2$ for the $y$-orientation ($B||y$). The experimental spectrum is shown on the top of the figure. The intense line corresponds to the even isotope with $I = 0$. The calculated spectra for isotopes Yb$^{3+}$ (171) ($I = 1/2$) and Yb$^{3+}$ (173) ($I = 5/2$) are shown on the bottom. The arrows show lines not related to the single ion spectrum.
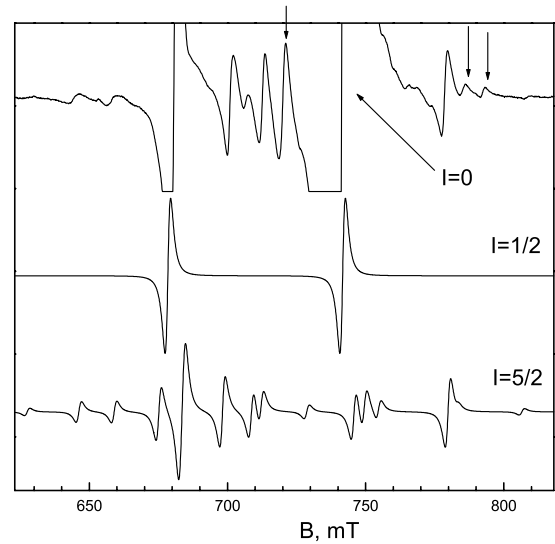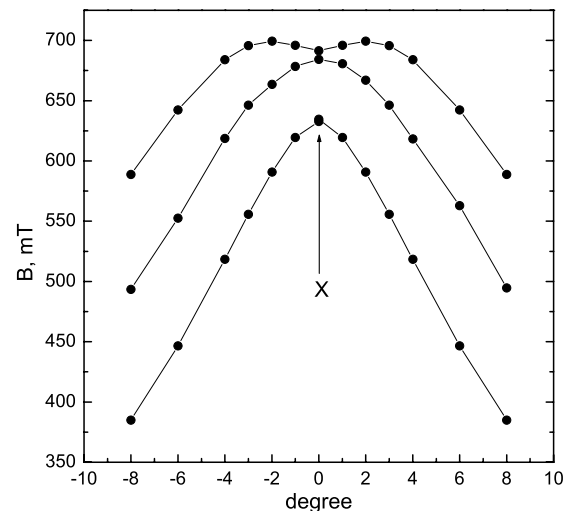
parameters are equal to zero for even isotopes, and in this case the spectrum consists of one intensive absorption line described by the first term of (1). The angular dependence of the $g$-factor is described by the standard expression:

$$g^2 = g_z^2 \cos^2 \Theta + g_x^2 \sin^2 \Theta \cos^2 \varphi + g_y^2 \sin^2 \Theta \sin^2 \varphi$$

where $\Theta$ and $\varphi$ are the polar and azimuthal angles, respectively, determining the direction of external magnetic field in coordinate system coinciding with the directions of the principal values of the $g$-tensor.

The spectrum of the isotope with the nuclear spin $I = 1/2$ consists of two lines of hyperfine structure and is described by the spin Hamiltonian (1) with two first members only, since for $I = 1/2$ the quadrupolar moment is equal to zero. The $g$-factor of this isotope is the same as for isotopes with $I = 0$.

In the $z$ orientation both lines of the hyperfine structure are placed almost symmetrically relative to the single resonance lines for even isotopes, while in the $x$ and $y$ orientations the asymmetry in their arrangement is observed. It is caused by large anisotropy of both the $g$-factor and the hyperfine interaction constant. The angular dependences of the EPR spectrum near the $x$ and $y$ orientations are shown in Figures 4 and 5, respectively. The high field resonance line of hyperfine structure coincides with the intensive line for the even isotopes.



**Fig. 4.** The angular dependence of the Yb$^{3+}$ion EPR spectrum in KY(WO$_4$)$_2$ for isotope with $I = 1/2$ near the $x$-orientation. The open circles represent the angular dependence for the even isotopes ($I = 0$). The interval between experimental points is equal to $1°$ for axis of abscissa.
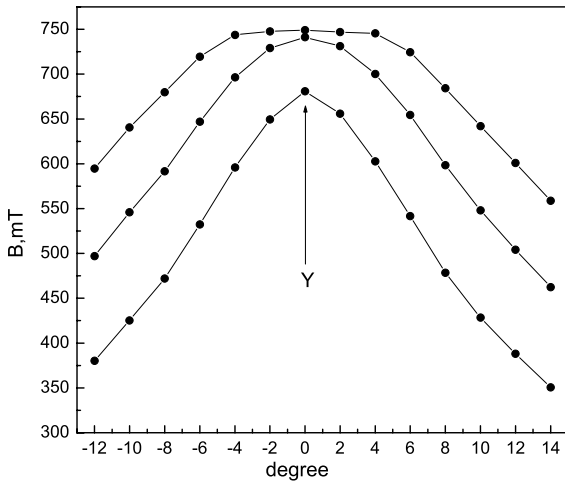
**Fig. 5.** The angular dependence of the EPR spectrum of $Yb^{3+}$ ion in $KY(WO_4)_2$ for isotope with $I = 1/2$ near the $y$-orientation. The angular dependence from the even isotopes ($I = 0$) is in the central part of the spectrum. The interval between experimental points is equal to $1°$ for abscissa axis.

The isotope with nuclear spin $I = 5/2$ produces the most complex spectrum. The six lines of hyperfine structure in the $z$ orientation are almost equidistant and are located symmetrically relative to the absorption line for even isotopes. The additional absorption lines are also observed between 1 and 2 and between lines 5 and 6 of the hyperfine structure. The solution of the Hamiltonian (1) has shown that an occurrence of the additional lines in the $z$ orientation is possible when the non-diagonal $P_{zx}$ component of the quadrupolar interaction $P$ tensor is non-zero. In this case the $P$ tensor should be diagonalized in the coordinate system turned relative to the $g$- and $A$-tensors in the $ac$ plane. The turning angle is about five degrees.

The values of hyperfine and quadrupolar interaction constants in the $x$ and $y$ orientations are the same order, so there is additional mixing of the quantum states that complicates the spectrum. The resonance lines related to "hyperfine" or "quadrupolar" transitions are difficult to distinguish in the way possible in the $z$ orientation. The spectra for different angles near the $x$ orientation calculated using Hamiltonian (1) are shown in Figure 6. These spectra demonstrate strong mixing of quantum states.

In the central part of the spectrum near the lines for the even isotopes there are additional resonance lines, which are not described by Hamiltonian (1). We assume that these lines correspond to spin-spin interactions between nearest neighbors Yb ions, which can form Yb-Yb pairs. Such additional lines were also observed in the EPR spectra of the Dy [9] and Er ions [7].

In order to compare the $g$-factor directions with respect to the crystallographic axes for different rare earth ions, single crystals doped by a small amount of $Yb^{3+}$, $Er^{3+}$ and $Dy^{3+}$ ions have been synthesized. The angular dependences of the resonance fields along the $z$-axis for each spectrum are presented in Figure 7. The angle
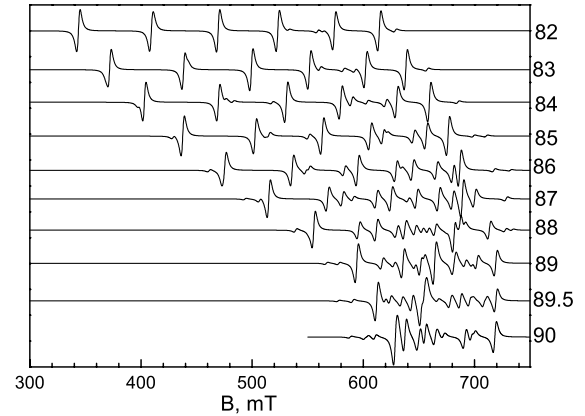


**Fig. 6.** The angular dependence of the EPR spectrum of $Yb^{3+}$ ion in $KY(WO_4)_2$ near the $z$ orientation for isotope with $I = 5/2$. The angle value of $90°$ corresponds to the $B \| x$ direction. The calculation was made using the parameters given in the manuscript.
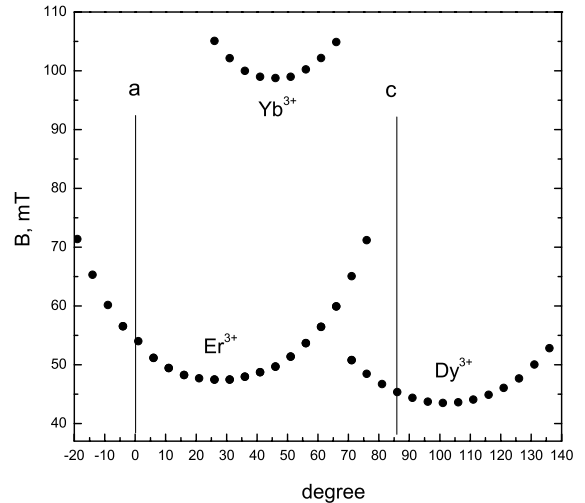


**Fig. 7.** The angular dependences of the EPR (for even isotope) spectra for the $Er^{3+}$, $Dy^{3+}$, $Yb^{3+}$ ions in the $ac$ plane with respect to the crystallographic axes (for symmetry I2/c) in $KY(WO_4)_2$ crystal. The interval between experimental points is equal to $5°$ for abscissa axis.

between the $z$ axes for $Yb^{3+}$ and $Er^{3+}$ ions is equal to $17° \pm 1°$, for $Yb^{3+}$ and $Dy^{3+}$ ions is $57° \pm 1°$, for $Er^{3+}$ and $Dy^{3+}$ ions is $74° \pm 1°$. In Figure 7, the $a$ and $c$ axes correspond to I2/c space group. The angle between the $z$- and $c$-axes for the $Yb^{3+}$ ion is $42° \pm 3°$. These results clearly show the effect inherent to the low symmetry, namely, the rotating of the $g$-factor axes for different rare earth ions in the $ac$ plane.

## 4 Temperature dependence of EPR spectra

The rare earth ions with unfilled $4f$ shell are strongly affected by lattice fluctuations (except for the $Gd^{3+}$ ion with $^8S_{1/2}$ configuration). As a result, these ions have
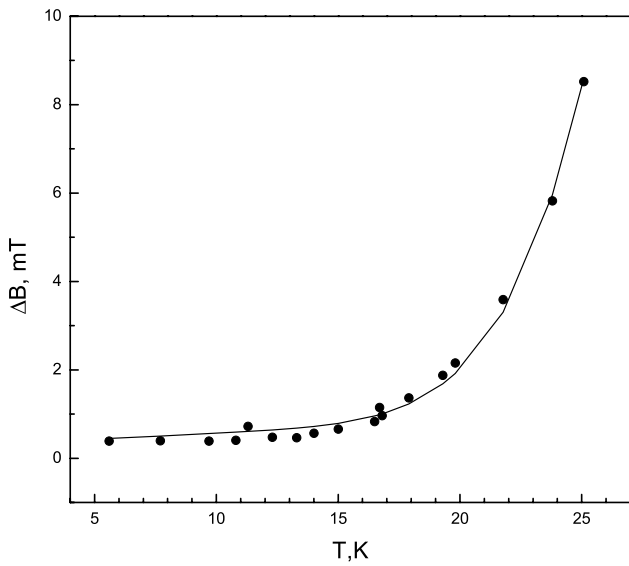
**Fig. 8.** The temperature dependence of the EPR linewidth for even isotope of the Yb$^{3+}$ ion. The solid line represents the best fitting of equation (2) to the experimental points.



**Fig. 9.** The temperature dependence of the $g$-factor of the Yb$^{3+}$ ion in the $z$ orientation.

short spin-lattice relaxation times, and the EPR spectra can be observed at low temperature only. At higher temperature ($T > 40$ K) the absorption line becomes unresolved due to its broadening. The study of the temperature dependence of the linewidth by EPR allows evaluation of spin-lattice relaxations times and thus establishes the mechanisms of spin-lattice relaxation. The measurements have been performed in the $z$-orientation. The resonance linewidth was measured as the distance between two peaks of the absorption line derivative. The linewidth versus temperature for the most intensive line in the spectrum for even isotopes is shown in Figure 8. The spin-phonon contribution to the linewidth was evaluated by subtracting from the total linewidth value the value of temperature-independent linewidth obtained at the lowest temperature. The experimental temperature dependence of the spin-lattice relaxation time can be described by superposition of direct and combinational processes

$$T_1^{-1} = 7.6 \times 10^6 T + 7.2 \times 10^{-4} T^9 f\left(\frac{\Theta}{T}\right) \qquad (2)$$

where $T_1^{-1}$ is the relaxation rate in s$^{-1}$ connected with the spin-phonon contribution to the linewidth $\Delta B$ by the relation $T_1^{-1} = 1.4 \times 10^7 \pi g \Delta B$, the temperature in Kelvin, $\Theta_D$ the Debay temperature,

$$f\left(\frac{\Theta}{T}\right) = \int_0^{\Theta/T} \frac{x^8 e^x}{(e^x - 1)^2} dx \ [17].$$

The Debay temperature is 280 K (193 cm$^{-1}$) [18], therefore in the experimental range of temperatures ($\Theta \gg T$) the function $f(\Theta/T)$ is practically equal to 1.

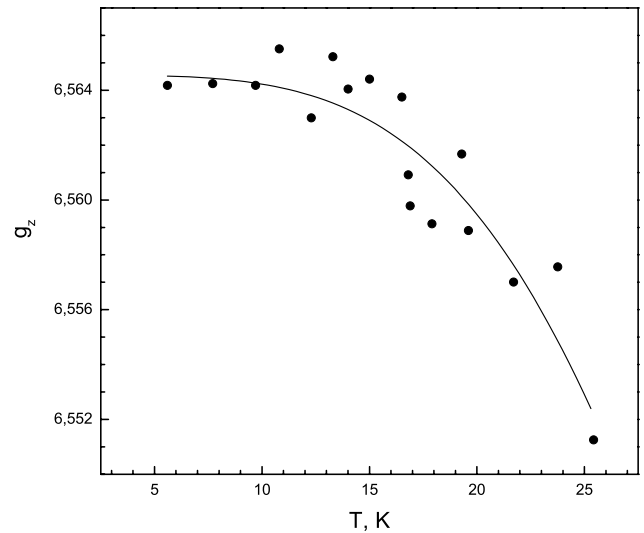A comparison between the spin-lattice relaxation time $T_1$ for the Yb$^{3+}$ ions and values of $T_1$ for the Dy$^{3+}$ and Er$^{3+}$ ions [7,8] in the same crystals shows that relaxation processes for the Yb$^{3+}$ ions differ essentially. Relaxation through the excited levels (Orbach relaxation) is characteristic for the Dy$^{3+}$ and Er$^{3+}$ ions, because the first excited energy level is located very close to the ground state: $-9.4$ cm$^{-1}$ and 36 cm$^{-1}$ for the Dy$^{3+}$ and Er$^{3+}$ ions, respectively. The first excited level of the Yb$^{3+}$ ion is located considerably higher from the ground state (168 cm$^{-1}$), so that for this ion the Orbach relaxation processes are not effective.

The experimental EPR line not only broadens with increasing temperature, it also changes position. This means that the $g$-factor for the Yb$^{3+}$ ion is temperature dependent. The temperature dependence of the fine and hyperfine structure constants describing EPR spectra is well known. Similar behavior of the $g$-factor with temperature was reported earlier [6,7,11]. The temperature dependences of the g-factor for the Yb$^{3+}$ ion in the $z$ and $x$ orientations in a temperature range of 4–25 K are presented in Figures 9 and 10. At $T > 25$ K, the absorption line is strongly broadened, and the measurements of both the linewidth and $g$-factor become unreliable. Assuming that phonon distribution is described by the Debay model, then a change of the $g$-factor with temperature, as well as other parameters of spin Hamiltonian, should be proportional to

$$T^4 \int_0^{\frac{\Theta}{T}} \frac{x^3 dx}{e^x - 1} \ [19\text{--}21],$$

where $x = h\nu/(kT)$, $h$ is the Planck constant, $\nu$ the phonon frequency, $k$ the Boltzmann constant. Since the Debay temperature is relatively high for double tungstates, the integral at $T^4$ in the investigated range is temperature-independent. The fitting lines proportional to $T^4$ are shown in Figures 9 and 10.
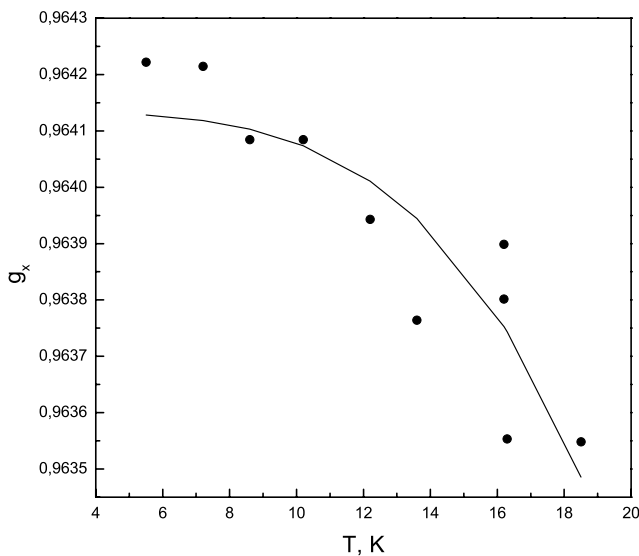
**Fig. 10.** The temperature dependence of the $g$-factor of the Yb$^{3+}$ ion in the $x$ orientation.

The experimental temperature dependences of the $g$-factor for studied rare earth ions in double tungstates can be divided into two subgroups depending on the magnitude of the $g$-factor shift: Dy$^{3+}$, Er$^{3+}$ and Yb$^{3+}$. The relative change of $g$-factors for these subgroups in the same temperature range differs essentially. The value of $\Delta g/g\ \Delta T$ for Dy$^{3+}$ ion is $1.8 \times 10^{-3}$, for Er$^{3}$ ion — $2.2 \times 10^{-3}$ and for Yb$^{3+}$ — $7.3 \times 10^{-5}$. Thus, the $\Delta g/g\ \Delta T$ values in the subgroups differ by almost two orders of magnitude. Note that the $g$-factor for rare-earth ions decreases as temperature increases. Since the lattice vibrations do not affect the Kramers doublet directly, their influence arrives throughout the admixture of excited spin states. The mixing is stronger if the distance between the ground and excited states is smaller, for example, for Dy$^{3+}$ and Er$^{3+}$ions in comparison with the Yb$^{3+}$ ion. Therefore a spin-lattice relaxation for Dy$^{3+}$ and Er$^{3+}$ions is more efficient than for Yb$^{3+}$. Close-lying excited levels promote of the Jahn-Teller effect even in a low symmetry crystal, such as KDy(WO$_4$)$_2$ [22,23].

At the present time there is no theoretical explanation of temperature dependence of the $g$-factors for ions with quenched orbital moments. The change of spin Hamiltonian parameters with temperature can be described formally by means of spin-phonon Hamiltonian used in references [19–21,24]. However, a large number of parameters in this Hamiltonian (especially, for monoclinic symmetry) and difficulties of their determination make this problem practically unresolved.

## 5 Conclusions

Paramagnetic Yb$^{3+}$ ions replacing diamagnetic Y$^{3+}$ ions in the monoclinic single crystal KY(WO$_4$)$_2$ show strong magnetic anisotropy. The discrepancy between the nuclear quadrupolar interaction tensor axis and the axes of both $g$-tensor and magnetic hyperfine interaction tensor leads to occurrence of additional "quadrupolar" resonance lines in the EPR spectra. Comparable values of quadrupolar and magnetic hyperfine interactions parameters in the $x$- and $y$-orientations lead to strong mixing of quantum states. The low crystal symmetry forces a rotatation of the $g$-tensor axes for different trivalent ions replacing yttrium.

The broadening of the resonance lines with increasing temperature is connected with the short spin-lattice relaxation times caused by combinational phonon scattering processes. The low temperature dependence of the $g$-factor at low temperatures is caused by the presence of the strong spin-orbital and orbital-lattice couplings.

## References

1. A.A. Kaminskii, P.V. Klevtsov, L. Li, A.A. Pavlyuk, Phys. Stat. Sol. A **5**, K79 (1971)
2. A.A. Kaminskii, A.F. Konstantinova, V.P. Orekhova, A.V. Butashin, R.F. Klevtsova, A.A. Pavlyuk, Crystallography Reports **46**, 733 (2001)
3. A.A. Kaminskii, *70 years researches of Raman scattering* (Fiz In-t RAN, Moscow, 1998), p. 206
4. A. Major, J.S. Aitchison, P.W.E. Smith, N. Langford, I. Ferguson, Opt. Lett. **29**, 1 (2004); A.S. Kumaran, A.L. Chandru, S.M. Babu, M. Ichimura, J. Crystal Growth. **275**, e1901 (2005); A.S. Kumaran, A.L. Chandru, S.M. Babu, I. Bhaumik, S. Ganesamoorthy, A.K. Karnal, V.K. Wadhawan, M. Ichimura, J. Crystal Growth. **275**, e2117 (2005)
5. A.A. Lagatsky, A. Abdolvand, N.V. Kuleshov, Opt. Lett. **25**, 616 (2000); M.C. Pujol, X. Mateos, R. Sole, J. Massons, J. Gavalda, X. Solans, F. Diaz, M. Aguilo, J. Appl. Crystallography **35**, 108 (2002)
6. M.T. Borowiec, V. Dyakonov, V. Kamenev, I. Krygin, S. Piechota, A. Prokhorov, H. Szymczak, Phys. Stat. Sol. (b) **209**, 443 (1998)
7. M.T. Borowiec, V. Dyakonov, A. Prokhorov, H. Szymczak, Phys. Rev. B **62**, 5834 (2000)
8. M.T. Borowiec, A.A. Prokhorov, A.D. Prokhorov, V.P. Dyakonov, H. Szymczak, J. Phys.: Condens. Matter. **15**, 5113 (2003)
9. M.T. Borowiec, A.D. Prokhorov, I.M. Krygin, V.P. Dyakonov, K. Wozniak, L. Dobrzycki, T. Zayarnyuk, M. Baranski, W. Domuchovski, H. Szymczak, Physica B **371** 205 (2006)
10. I.M. Krygin, A.D. Prokhorov, V.P. Dyakonov, M.T. Borowiec, H. Szymczak, Physics of the Solid State **44**, 1587 (2002)

11. I.M. Krygin, A.D. Prokhorov, V.P. Dyakonov, M.T. Borowiec, H. Szymczak, Physics of the Solid State **45**, 2083 (2003)
12. P.V. Klevtsov, L.P. Kozeeva, R.F. Klevtsova, Inorganic Material **4**, 1147 (1968)
13. S.V. Borisov, R.F. Klevtsova, Crystallography Reports **13**, 517 (1968)
14. J.K. Viscakas, I.V. Mochalov, A.V. Mikhailov, R.F. Klevtsova, A.V. Lyubimov, Soviet Physics Collection **28**, 64 (1988) [Original: Litovskii-Fizicheskii-Sbornik. **28**, 224 (1988)]
15. C. Zaldo, M. Rico, C. Cascales, M.C. Pujol, J. Massons, M. Aguilo, F. Diaz, P. Porcher, J. Phys.: Condens. Matter. **12**, 8531 (2000)
16. M.C. Pujol, M.A. Bursukova, F. Guell, X. Mateos, R. Sole, Jna. Gavalda, M. Aguilo, J. Massons, F. Diaz, F. Klopp, U. Griebner, V. Petrov, Phys. Rev. B **65**, 165121 (2002); M.C. Pujol, M. Aguiló, F. Díaz, M.T. Borowiec, A.D. Prokhorov, V.P. Dyakonov, A. Nabialek, S. Piechota, H. Szymczak, Physica B, 2006 (to be published)
17. A. Abragam, B. Bleaney, *Electron Paramagnetic Resonance of Transition Ions* (Clarendon Press, Oxford, 1970), Vol. 1
18. A. Szewczyk, M.U. Gutowska, K. Piotrowski, M. Gutowski, M.T. Borowiec, V. Dyakonov, V.L. Kovarskii, H. Szymczak, L. Gladczuk, J. Phys.: Condens Matter. **10**, 10539 (1998)
19. C.A. Bates, H. Szymczak, Phys. Stat. Sol. (b) **74**, 225 (1976)
20. C.A. Bates, H. Szymczak, Z. Phys. B **28**, 67 (1977)
21. K.H. Srivastava, Physics Report. **20**, 3137 (1975)
22. M.T. Borowiec, V. Dyakonov, A. Jedrzejczak, V. Markovich, A. Nabialek, A. Pavlyuk, S. Piechota, A. Prokhorov, H. Szymczak, Sol. St. Comm. **102**, 627 (1997)
23. I.M. Krygin, A.D. Prokhorov, Soviet Physics JETP **86**, 590 (1984)
24. S.A. Altshuler, B.M. Kozyrev, *Electronic Paramagnetic Resonance* (Nauka, Moscow, 1972)